# HEAVY QUARK AND JET PRODUCTION BY REAL AND VIRTUAL PHOTONS

F. SEFKOW
*Physik-Institut der Universität Zürich*
*CH-8057 Zürich, Switzerland*

Recent results from the H1 and ZEUS collaborations on hard QCD processes in $ep$ interactions are reviewed. The topics cover jet shapes, the structure of real and virtual photons, and the production of $J/\Psi$ mesons and open charm.

## 1 Introduction

Heavy flavours and jets in the hadronic final state carry much information about the dynamics of the unobservable quarks and gluons. They thus provide access to the underlying hard partonic processes of high energy $ep$ interactions. The aim is to test the description of the production processes by perturbative QCD, and to extract information on the parton distributions of the initial state hadron.

At HERA, electrons (or positrons) of 27.5 GeV collide with 820 GeV protons, the center-of-mass energy is $\sqrt{s} = 300$ GeV. The bulk of the scattering reactions occur in the photoproduction regime where the momentum transfer $Q^2 \approx 0$, i.e. the exchanged photon is almost real; data in the Deep Inelastic Scattering (DIS) regime correspond to large $\gamma$ virtualities $Q^2 >> 1$ GeV$^2/c^2$. In both regimes, however, the $\gamma p$ center-of-mass energies $W$ are typically as high as $\approx$ 100 - 200 GeV and open up the phase space for hard QCD processes. The HERA experiments H1 and ZEUS thus extend the range of fixed-target photoproduction experiments by an order of magnitude.

This review begins with results from the study of jets in photoproduction and DIS, the focus is on the structure of both real and virtual photons. In the second part, the production of bound and open charm states will be discussed in terms of perturbative QCD models.

## 2 Jets in Photoproduction

In Leading Order QCD, a photon can either interact directly with a parton in the proton ("direct" photoproduction, $\gamma q \rightarrow qg$ and $\gamma g \rightarrow q\bar{q}$), or it can fluctuate into a quark-antiquark pair, which may form a vector meson state or may develop a quark-gluon structure without forming a hadronic bound state ("anomalous " characteristics of the photon). A parton from that state

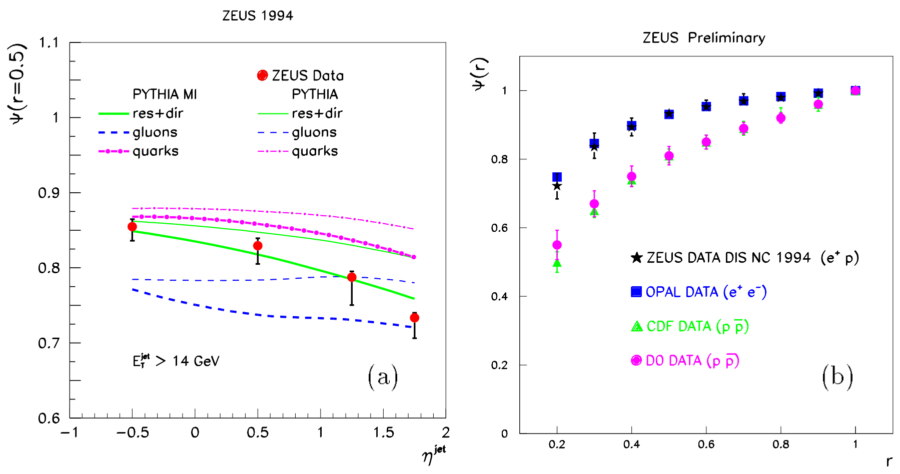


Figure 1: Jet shape (fraction of transverse energy in a sub-cone of radius $r$) for a jet defined by a cone of radius $R = 1$, (a) in photoproduction, at fixed $r = 0.5$ as function of rapidity, (b) in DIS at HERA, as function of $r$, compared with LEP and Tevatron data.

interacts with a parton from the proton ("resolved" photoproduction; most important are $qq' \to qq'$, $qg \to qg$ and $gg \to gg$). Since the parton carries only a fraction $x_\gamma$ of the photon's momentum, the "resolved" events at HERA exhibit a stronger boost into the proton ("forward") direction, towards positive pseudo-rapidities $\eta$.[a]

### *2.1 Jet Shapes*

A necessary prerequisite for the interpretation of jet photoproduction data in partonic terms is being able to model the internal structure of hadron jets. Let the jet be defined by a cone algorithm which combines hadrons within a cone of radius $R$, measured in the $(\eta, \phi)$ plane. A suitable quantity to describe the jet shape is $\Psi(r)$, defined as the fraction of the jet's transverse energy contained in a sub-cone of radius $r$. $\Psi(r)$ increases towards 1 with $r$ approaching $R$; the more collimated the jet, the steeper the rise and the higher $\Psi$ at fixed $r$.

In Fig. 1a $\Psi(r = 0.5)$ as measured by ZEUS [1] is displayed as a function of the jet pseudo-rapidity $\eta$, for jets with transverse energy $E_\perp > 14$ GeV and $R = 1$. The result clearly shows that the jets are broader in the forward region. Predictions of the QCD Monte Carlo program PYTHIA [2] are shown

[a] The pseudo-rapidity is defined as $\eta = -\ln\tan(\theta/2)$, where $\theta$ is the polar angle measured with respect to the $z$ axis, taken to be along the direction of the incident proton beam.

for comparison. The thick curve which gives the best description of the data. has been obtained with the inclusion of multi-parton interactions in "resolved" processes. The predictions are also shown separately for jets initiated by either quarks or gluons. Gluon jets are broader since they have higher color charge so that QCD radiation is more likely to occur. In the generator program, the average broadening with $\eta$ can be traced to an increased fraction of gluon-initiated jets, which in turn is due to the increased contribution of "resolved" events in the forward direction.

It is interesting to note that in DIS, at high $Q^2 > 100$ GeV$^2/c^2$, the jet shapes measured at HERA [1] agree very well with those observed at LEP [3] (Fig. 1b). This is expected in the quark parton model, where a quark is "kicked" out of the proton and produces the jet. The function $\Psi(r)$ exhibits a distinctly steeper rise than that observed in $\bar{p}p$ interactions [4], where predominantly gluon initiated jets are produced.

Jet shapes in photoproduction have also been calculated analytically using Next to Leading Order (NLO) QCD matrix elements [5]. In order to emulate effects of the experimental jet finding procedures, a parameter $R_{sep}$ has to be introduced into the theoretical calculation; $R_{sep}$ specifies the maximum distance of two partons to be merged into one jet. Given the freedom in this jet finding parameter, the measured jet shapes can be reproduced.

### *2.2 Dijet angular distribution*

In the Leading Order (LO) picture, the kinematics of the partonic $2 \to 2$ process can be fully reconstructed in dijet events from the jets' energies and angles. Such an analysis can reveal dynamical features of the strong interactions mediating the jet production.

One defines an observable related to the momentum fraction of the parton in the photon, $x_\gamma^{OBS} = \sum_{jets} E_\perp^{jet} \exp(-\eta^{jet})/2yE_e$ where $E_e$ is the $e$ beam energy, and $y = 1 - E_\gamma/E_e$ can be obtained from the scattered electron or from all final state hadrons. For the scattering angle in the partonic center-of-mass system one has $\cos\theta^* = \tanh(\eta^{jet\,2} - \eta^{jet\,1})/2$. Although beyond LO only the sum of "direct" and "resolved" processes can be unambiguously defined, and the $2 \to 2$ kinematics formulae do not apply exactly anymore, these quantities – being defined as hadronic observables – are meaningful at any order.

The uncorrected $x_\gamma$ distribution from ZEUS [6] is shown in Fig. 2a. It is qualitatively reproduced by the Monte Carlo calculations shown in the same figure. For direct processes, $x_\gamma^{OBS}$ is expected to be close to 1. The data is thus split into a "direct" sample ($x_\gamma > 0.75$) and a "resolved" sample ($x_\gamma < 0.75$).

In QCD, the dominant Leading Order diagrams for direct processes involve

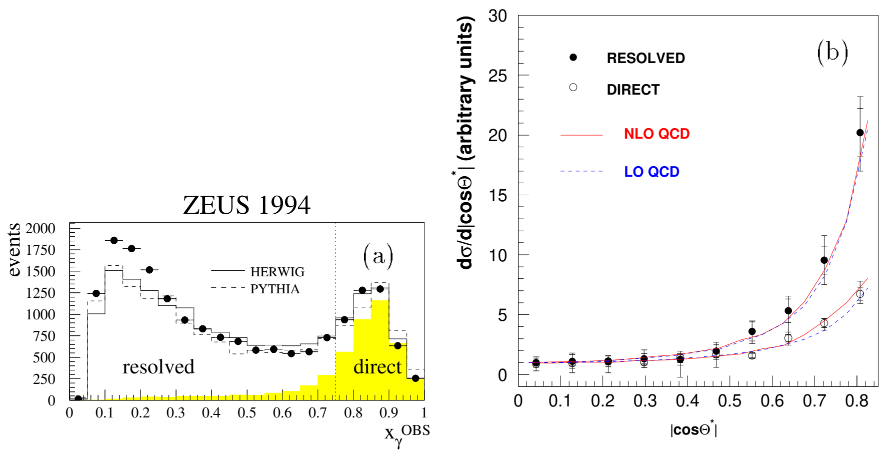


Figure 2: (a) Uncorrected $x_\gamma^{OBS}$ distribution for dijet events. (b) Dijet angular distribution in the parton parton center-of-mass system.

quark (spin $\frac{1}{2}$) exchange, whereas for the "resolved" case, gluon exchange (spin 1) dominates. The angular distributions are thus predicted to be different: $\sim |1 - \cos\theta^*|^{-1}$ in the first case, and a steeper $|1 - \cos\theta^*|^{-2}$ behavior in the latter. This expectation is nicely confirmed by the ZEUS measurements [6] shown in Fig 2b. The distributions reflect the spin of the exchange as well as the relative contributions of direct and resolved processes to each sample. Moreover, NLO calculations [7] exhibit the same pattern and also agree well with the data.

### *2.3 Photon Structure*

The jet cross sections evidently depend on the parton distributions in the photon. At HERA, the proton acts as hadronic probe, and the data are sensitive to both the quark and the gluon content of the photon. The measurements have provided the first determination of the gluon momentum distribution by H1 [8]. The recent analysis presented here [9] investigates the scale dependence of the parton distribution and confronts it to QCD predictions.

H1 has measured the double differential dijet cross section as a function of $x_\gamma^{OBS}$ and $E_T^2$, the second highest transverse jet energy squared, in the range $0.1 < x_\gamma < 1$ and $E_T^2 > 8$ GeV$^2$. The data have been analyzed in terms of an effective parton distribution – i.e. not differentiating quarks and following the concept of Ref. [10]. This is possible since the most important leading order matrix elements in "resolved" photoproduction have angular distributions

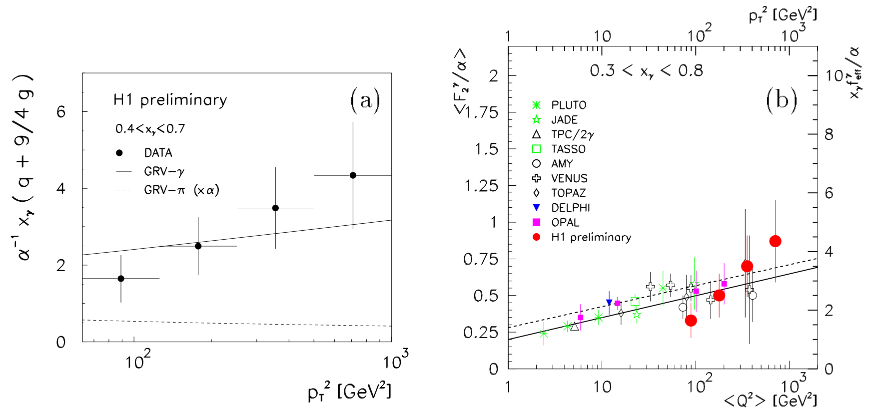


Figure 3: (a) Scale dependence of the effective parton density $f^{\gamma}_{eff}$ of the photon. (b) Dependence of the photon structure function $F_2^{\gamma}$, measured in two photon reactions, on the scale given by the virtuality $Q^2$ of the probing photon. $f^{\gamma}_{eff}$ was divided by 5 (see text) and is shown as function of the scale given by the parton transverse momenta $p_t^2$ [12]. The lines represent calculations in the FKP model[14] with different parameter settings.

similar in shape, they mainly differ in overall magnitude by the ratio of color factors. Consequently, the cross section can be described by means of a single effective subprocess with matrix element $|M_{SES}|^2$. One defines *effective* parton distributions for photon *and* proton:

$$f_{eff}(x,p_\perp^2) = \sum_{flavours} (q(x,p_\perp^2) + \bar{q}(x,p_\perp^2)) + \frac{9}{4} g(x,p_\perp^2) \quad , \tag{1}$$

where $q$ and $g$ denote the quark and gluon densities, respectively, $x$ the momentum fraction and $p_\perp^2$ the factorization scale of the process given by the parton's transverse momentum squared. The dijet cross section then factorizes to good approximation, symbolically:

$$\sigma \sim f^{\gamma}_{eff}(x_\gamma, p_\perp^2) \cdot f^{p}_{eff}(x_p, p_\perp^2) \cdot |M_{SES}|^2 \quad . \tag{2}$$

The effective parton distribution $f^{\gamma}_{eff}$ extracted from the double differential cross section is shown in Fig. 3a as function of the scale $p_\perp^2$ for the range $0.4 < x_\gamma < 0.7$. The data clearly show a direct dependence on the scale; This positive scaling violation is remarkably different from the behavior of hadronic structure functions, where the dependence on the scale enters only via the QCD evolution equations and, at large momentum fractions, is negative. For comparison the GRV parameterization [11] of the photon structure is shown (full line). In a vector meson dominance picture the effective parton density would be proportional to a vector meson structure function; here the effective parton density of the pion is shown, scaled by the probability of the photon fluctuating into a vector meson. this is also shown for comparison as the dashed line. The behavior of the photon is a genuine QCD prediction. It originates from the inhomogeneous term in the Altarelli-Parisi evolution equations which is only present for the photon, due to its point-like coupling to quarks, and is referred to as its "anomalous component".

The H1 result ties in nicely with the scaling behavior of the photon structure function $F_2^\gamma$ as determined in two-photon experiments, where a highly virtual photon probes the quark content of a real photon. QCD predicts the scaling to be $F_2^\gamma \sim \ln Q^2/\Lambda^2_{QCD}$. A similar dependence can be expected for $f^\gamma_{eff}$ at large $x_\gamma$, since here the gluon contribution to it is small according to the H1 measurement [8]. From the GRV parameterization of quark and gluon distributions, the ratio $f^\gamma_{eff}/F_2^\gamma$ is expected to be about 5 and approximately constant. Fig. 3b [12] shows the H1 result, scaled by this factor, overlaid onto a compilation of $F_2^\gamma$ results from $e^+e^-$ experiments [13]. The HERA data are comparable in precision, and they extend the kinematic range towards a maximum scale of $p_\perp^2 = 1250\,\mathrm{GeV}^2/c^2$.

## 3 Jets in Deep Inelastic Scattering

In the previous section, it was discussed how the structure of the photon can be "resolved" by partons inside the proton. The "resolution" is given by the hard scale of the partonic sub-process, e.g. the transverse energy squared, $p_\perp^2$. On the other hand, deep inelastic $ep$ scattering (DIS) is usually described in the quark parton model, where a virtual, point-like photon probes the structure of the proton, the "resolution" being given by the negative 4-momentum transfer $Q^2$. In the kinematic regime of DIS, where $Q^2$ is low, but there is another hard scale $p_\perp^2 > Q^2$ present, it is an open question whether this is still an adequate description. HERA offers the possibility to probe this interesting transition region between DIS and the photoproduction limit.

### *3.1 Dijet Rates*

2+1 jet (dijet) events[b] in QCD are due to $\mathcal{O}(\alpha_s)$ processes, namely radiation of a hard gluon off the scattered quark (QCD-Compton), or boson gluon fusion (BGF). At low $Q^2 < 100$ GeV$^2/c^2$, BGF is strongly dominant.

[b] The proton remnant jet is counted separately as "+1".

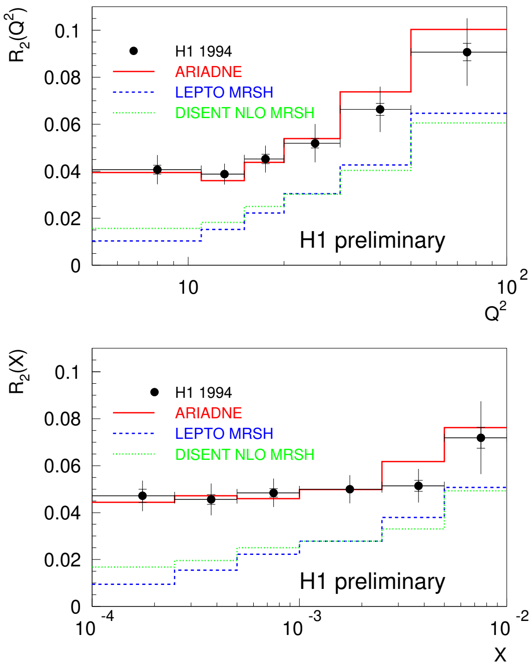


Figure 4: Dijet rate in DIS as function of $Q^2$ and $x_{Bj}$, compared to ARIADNE (full histogram), LEPTO (dashed) and DISENT (light dashed) calculations.

The dijet rate $R_2$ measured by H1 [15] is shown in Fig. 4 as a function of $Q^2$ and the Bjorken scaling variable $x_{Bj}$. The jets were identified in the hadronic center-of-mass system by a cone algorithm with $R = 1$ and were required to have $E_T^* > 5$ GeV. Various predictions are compared to the data. The Color Dipole Model (CDM) as implemented in the ARIADNE [16] Monte Carlo program describes the data well. The LEPTO [17] Monte Carlo contains the exact LO ($\mathcal{O}(\alpha_s)$) matrix elements and parton showers in leading log approximation (MEPS). It falls short in describing the measured rate, in particular at lower $Q^2$. The same holds for a full NLO QCD calculation (DISENT [18]) where the jet algorithm is used to find jets from the final state partons. This discrepancy is unlikely to be an effect of missing hadronization effects, since these were found to be below 20% in the two Monte Carlo models.

The failure of the NLO calculation to reproduce the dijet rate may be an indication that higher order corrections are important in the kinematic region probed here. The CDM also predicts additional energy flow (hadronic activity) in the photon fragmentation region of the $\gamma p$ center-of-mass system, increasing as $Q^2$ decreases, whereas in the parton shower model, this quantity remains small and constant. The $Q^2$ dependence of the H1 data is reproduced by the CDM prediction [15]. It is possible to introduce additional processes with increased activity in this region into the conventional QCD models by allowing for a partonic structure of the virtual photon [19,20], analogous to the description of jet production by real photons. This will be investigated further in the future.

### *3.2 Virtual Photon Structure*

The parton densities in the virtual photon are expected in QCD to be suppressed with increasing virtuality $Q^2$; for $Q^2 > p_t^2$, the point-like component dominates. For example, according to the phenomenological ansatz of Drees and Godbole [20], following the analysis of Borzumati and Schuler [21], the $Q^2$-dependent suppression with respect to the densities in the real photon is parameterized as

$$f_{q|\gamma^*}(x, p_t^2, Q^2) = f_{q|\gamma}(x, p_t^2) \cdot L \quad \text{with} \quad L = \frac{\ln[(p_t^2 + \omega^2)/(Q^2 + \omega^2)]}{\ln[(p_t^2 + \omega^2)/\omega^2]} \tag{3}$$

The parameter $\omega$ controls the onset of the suppression. For gluons the suppression is stronger than for quarks ($\sim L^2$), since they have to be radiated off a parton that is already off-shell.

A study into this direction is the measurement of inclusive differential jet cross sections at lowest virtualities, in the region $0 < Q^2 < 50$ GeV$^2/c^2$ by H1 [22]. The jets are identified here by means of a $k_t$ clustering algorithm with a resolution scale parameter $E_{cut} = 3$ GeV. The measurement is expressed as a $\gamma^* p$ cross section, formally defined by dividing the $ep$ cross section by a flux factor given in the Weizsäcker-Williams approximation, thereby correcting for the trivial $Q^2$ dependence due to the photon propagator. The cross section as a function of the virtuality is shown in Fig. 5 for different regions of transverse jet energy. The data is compared to predictions obtained with the HERWIG Monte Carlo program [23], which includes in addition to the "direct", point-like process (shown as hatched histogram) a "resolved" contribution. The $\gamma^*$ parton densities are modeled with the Drees Godbole ansatz and $\omega = 1$GeV$^2/c^2$. Only the sum of the two contributions (full histogram) describes the data. The "resolved" component is found to be important in the kinematic region where the jet transverse energy $E_t^2 > Q^2$.

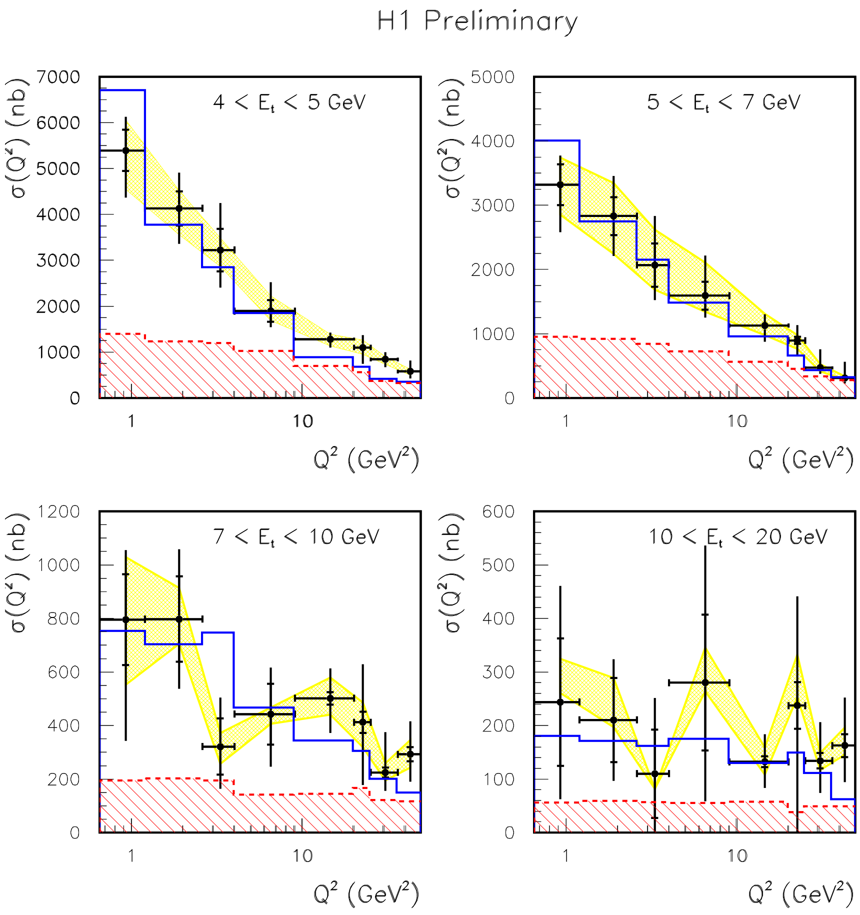


Figure 5: $\gamma^* p$ jet cross section as function of $Q^2$ in ranges of jet transverse energy.

## 4 Charm I: $J/\Psi$ Photoproduction

In the conventional picture of $ep$ interactions, charm is produced almost exclusively via boson gluon fusion. It is therefore considered as the "classical" way to probe the gluon content of the proton. This is one motivation to study the probing process more closely, but charm production is an interesting testing ground of perturbative QCD in its own right.

### *4.1 Elastic $J/\Psi$ Photoproduction*

Elastic $J/\Psi$ production offers a very clean experimental signature: the proton remains intact, the vector meson is detected in one of its leptonic decay channels, and apart from the $ee$ or $\mu\mu$ pair there is nothing else in the detector. The energy dependence of the cross section is a characteristic feature of the production dynamics. In Regge phenomenology, it is related to a Pomeron trajectory $\alpha(t) = 1+\lambda+\alpha' t$, where $t$ is the 4-momentum transfer to the proton [24]. The cross section behaves like

$$\sigma \sim \left(W^2\right)^{2\lambda} \quad ; \tag{4}$$

$\lambda$ is a universal constant for soft hadronic processes and of the order 0.08...0.1. On the other hand, it has been argued that due to the high mass of the $J/\Psi$ meson, perturbative QCD should be applicable. In the model of Ryskin *et al.* [25], the dominant diagram contains a gluon ladder, and the cross section is therefore proportional to the square of the gluon density in the proton:

$$\sigma \sim [xg(x)]^2 \quad \text{with} \quad x = M^2_{J/\Psi}/W^2 \quad . \tag{5}$$

Now the gluon density at low $x$ behaves like $xg(x) \sim x^{-\lambda}$; for the $W$ dependence again the form of Eq. 4 results, but $\lambda$ has a different meaning. The rise of the gluon density rather gives $\lambda$ values in the region 0.2...0.3. Thus, in this model a much steeper rise of the cross section with energy is expected.

At HERA, the Regge picture is beautifully confirmed by measurements of the total photoproduction cross section, and by detailed investigations of the elastic production of light vector mesons – see Fig. 6 and Ref. [26] for a recent overview. However, the rise of the elastic $J/\Psi$ cross section is found to be in clear disagreement with a soft Pomeron picture. This is now seen with the HERA data alone [27], for example, ZEUS find

$$4\lambda = 0.92 \pm 0.14 \pm 0.10 \quad . \tag{6}$$

The $W$ dependence can be well described by the (leading order) perturbative QCD calculation in the Ryskin *et al.* model, the agreement with experimental data is particularly good when the MRS(A$'$) [28] parameterization of the gluon density in the proton is used. The sensitivity to the gluon density is temptingly high in this model. However, recently there have also been suggestions to explain the steep rise of the $J/\Psi$ cross section within a modified soft Pomeron framework [29].

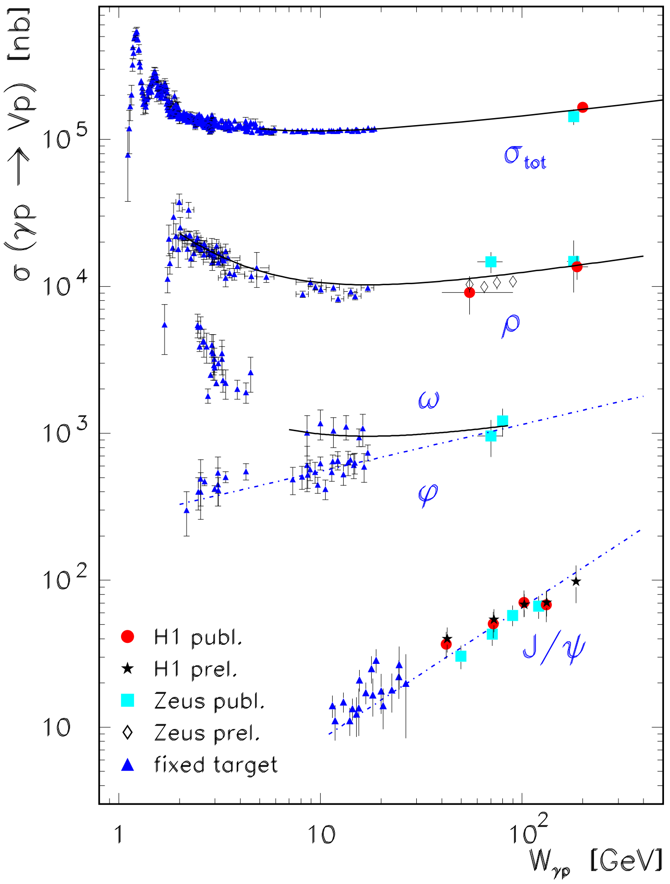


Figure 6: Total and elastic vector meson photoproduction cross section as function of CMS energy $W_{\gamma p}$. The solid lines are parameterizations based on Regge phenomenology.

### *4.2 Inelastic $J/\Psi$ Photoproduction*

Inelastic $J/\Psi$ production is described in the Color Singlet Model (CSM) [30] as production of a $c\bar{c}$ pair via boson gluon fusion. Another (relatively hard) gluon is radiated off one of the heavy quarks, in order to transform the pair into the color-neutral singlet state forming the $J/\Psi$ meson. Experimentally, the process can be separated by means of the elasticity variable $z$ that can be calculated from the longitudinal momenta of the $J/\psi$ products and of all final state particles: $z = (E - p_z)_{J/\psi}/(E - p_z)_{\text{all}}$. It represents, in the proton

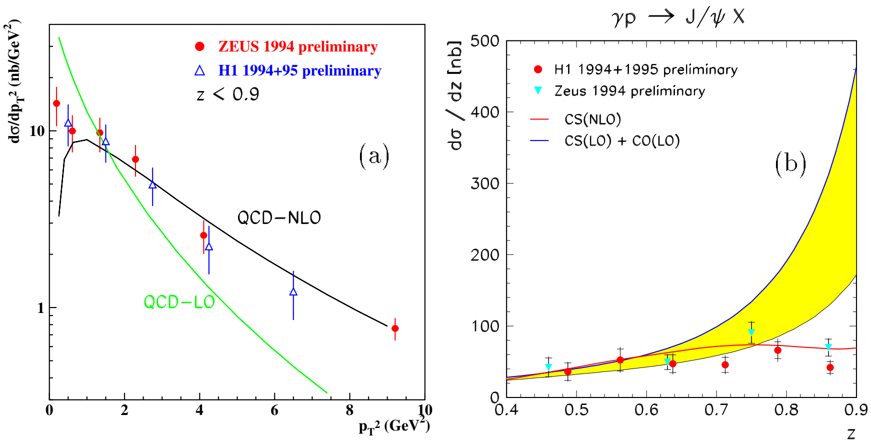


Figure 7: Cross section for inelastic $J/\Psi$ production as function of transverse momentum $p_t^2$ (a) and elasticity $z$ (b), compared to QCD calculations in the color singlet (CS) model (a) and CS and color octet (CO) model (b). The band indicates the theoretical uncertainty due to initial state radiation.

rest frame, the fraction of the photon's energy transferred to the $J/\Psi$ meson. Diffractive production leads to $z$ values close to 1, "resolved" contributions can be suppressed by a lower cut on $z$.

The differential cross section, measured by H1 and ZEUS [27] as function of the $J/\Psi$ transverse momentum squared is shown in Fig. 7a and compared to QCD calculations [31] in the CSM, in LO and NLO. Next to Leading Order corrections are substantial and clearly needed to reproduce the data. The parameters in the theoretical calculation (charm mass $m_c = 1.4$ GeV/$c^2$, renormalization and factorization scale $\mu = \sqrt{2}m_c$, and $\Lambda_{QCD} = 200$ MeV) are slightly "stretched"; other choices tend to give a lower cross section normalization and would leave room for additional production mechanisms. e.g. via fragmentation [32] or through color octet states.

Recently, the rôle of color octet contributions has been intensively discussed, as a possible explanation for the unexpectedly high $J/\Psi$ and $\Psi'$ production rates measured at the Tevatron [33]. In the factorization approach of non-relativistic QCD [34], $J/\Psi$ mesons can also be produced via color-octet $c\bar{c}$ configurations. The transition to the singlet final state is treated as a soft process described by non-perturbative matrix elements, which must be obtained from experimental data. They have been extracted [35] from the CDF $J/\Psi$ rates and yield a prediction for the HERA regime that can be confronted to data. The cross section measured by H1 and ZEUS is shown as a function of the elasticity $z$ in Fig. 7b. The color octet contributions are expected to enhance the cross section in the high $z$ region[36]. No indication for such an enhancement can be seen in the data yet. However, there are considerable theoretical uncertainties in the prediction. As an example, the band in the figure indicates the range of uncertainty due to an effective transverse momentum of the incoming partons, due to initial state radiation[37].

## 5 Charm II: $D^*$ Production

Open charm at HERA has mainly been reconstructed in the fragmentation and decay chain $c \to D^{*+} \to D^0\pi^+ \to (K^-\pi^+)\pi^+$ exploiting the clean experimental signal in the mass difference distribution of $m(K^-\pi^+) - m(K^-\pi^+)$.

### *5.1 $D^*$ Production by Real Photons*

The total open charm photoproduction cross section has been measured at HERA [38] at different photon proton center-of-mass energies up to $W \approx 230$ GeV and found to be an order of magnitude higher than at fixed target energies (Fig. 8). Together with a new point at "low" $W \approx 90$ GeV the data start to

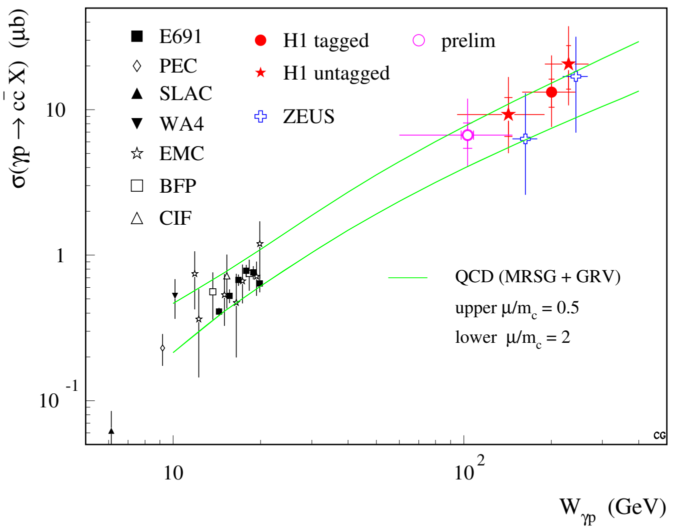


Figure 8: Photoproduction cross section as function of $Q^2$ in ranges of jet transverse energy.

provide some lever arm on the slope of the cross section versus energy, which is related to the $x$ dependence of the gluon density in the proton. However, there are large factors for the extrapolation (in $\eta$ and mainly $p_t$) from the visible to the total cross section involved, which depend on the parton densities in the proton and the photon. It is thus not straightforward to interpret the total cross section data in these terms.

Currently there exist two approaches to calculate differential distributions for $D^*$ photoproduction in NLO QCD. In the so-called "massive" charm scheme [40], charm quarks are treated as massive particles which are only generated perturbatively in the final state, whereas the 3 lightest flavours (and gluons) are the only active partons in the initial state proton and photon. This scheme is valid as long as $p_t$ is not too large with respect to the charm mass, and indispensable for the calculation of the total cross section. In contrast, in the "massless" scheme [41,42], charm is also an active flavour in the parton distributions of the proton and the photon. This scheme should work particularly well for large $p_t \gg m_c$; here, scale-dependent perturbative fragmentation functions are needed to control divergences. The "massless" scheme predicts a large ($> 50\%$) contribution of "resolved" processes of the type $cg \to cg$ initiated by a $c$ quark from the photon.[c] For comparison, the "resolved" component due to due to $gg \to c\bar{c}$, present in both approaches, is only of order 10%.

Differential cross sections as function of (pseudo-)rapidity and $p_t$ have been measured by H1 and ZEUS [38], with lower $p_t$ cuts at 2.5 or 3 GeV/$c$. The bulk of the data thus lies in a region where $p_t$ is neither particularly "small" nor "large". In Fig. 9a), the ZEUS results are compared to NLO QCD calculations in the two schemes. Within the – still large – experimental errors, the shape of the distribution is reproduced in both approaches. The normalization prefers the "massless' calculation, which has been performed using the Peterson-Zerwas form of the fragmentation function [43] with a fragmentation parameter $\epsilon_c = 0.064$ as it was obtained from fits to $e^+e^-$ data within the same framework. Within the "massive" scheme, such an analysis has not yet been performed; the parameter $\epsilon_c = 0.060$ is taken from a leading order analysis [44] of low energy $e^+e^-$ data. It has been argued [42] that rather a smaller value $\epsilon_c \approx 0.020$ would be consistent with the NLO calculation and reconcile it with the data.

In order to obtain further information on the production process, ZEUS has performed a dijet analysis similar to that described in Sec. 2.2 and measured the uncorrected $x_\gamma^{OBS}$ distribution for events containing a $D^*$ meson [39]. The jets were identified using a cone algorithm or – shown here – a $k_t$ cluster algorithm and were required to have transverse energy above 4 GeV. The result is shown in Fig. 9b and compared to the predictions of the HERWIG leading order

[c] This has no equivalent in the "massive" scheme, but one should bear in mind that only the sum of "direct" and "resolved" contributions is unambiguously defined at NLO.

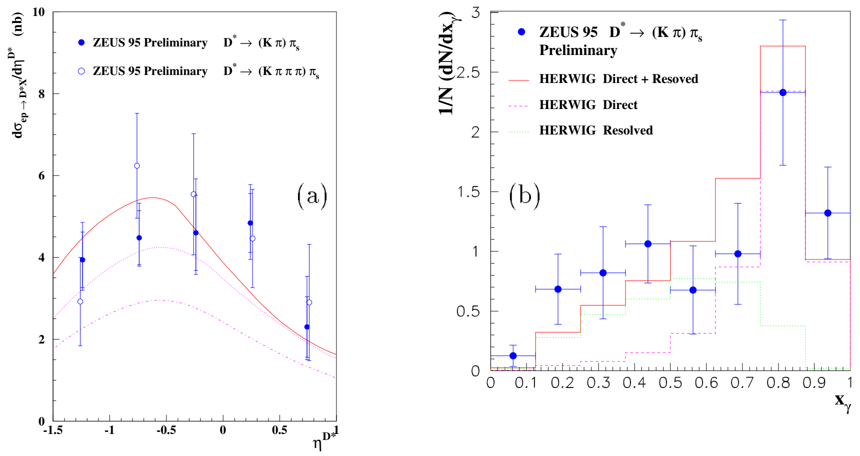


Figure 9: (a) Differential cross section for $D^*$ photoproduction as function of rapidity. The curves represent NLO QCD calculations in the "massless" (upper) and "massive" scheme, with default parameters (lower), and with charm mass $m_c = 1.5\,\mathrm{GeV}/c^2$ and scale $\mu = 0.5 m_c$ (middle). (b) Uncorrected $x_\gamma^{OBS}$ distribution for dijet events containing a $D^*$ meson.

Monte Carlo program. The data at lower $x_\gamma^{OBS}$ values need a substantial "resolved" photon contribution, which in the Monte Carlo is dominated by processes initiated by charm quarks from the photon.

### *5.2 $D^*$ Production by Virtual Photons*

In deep inelastic scattering, due to the recoil of the scattered electron, $D^*$ production can be measured in the full range down to $p_t = 0$ in the hadronic center-of-mass system, although a lower cut on the transverse momentum in the laboratory frame is usually necessary to suppress combinatorial background. The data is then dominated by $p_t \approx m_c$, so that one can expect a calculation in the "massive" scheme with 3 active flavours to provide a good description of the process in this regime. Fig. 10 demonstrates that this is indeed the case: the NLO calculation by Harris and Smith [45], performed in this scheme, agrees well with the data [46] in both magnitude and shape. One should also note that due to the smallness of the charm transverse momenta, $p_t^2 \ll Q^2$ is in general fulfilled, so that the virtual photon can be considered as a point-like probe to a good approximation. Deep inelastic charm production is therefore a very promising process to extract information about the gluon content of the proton.

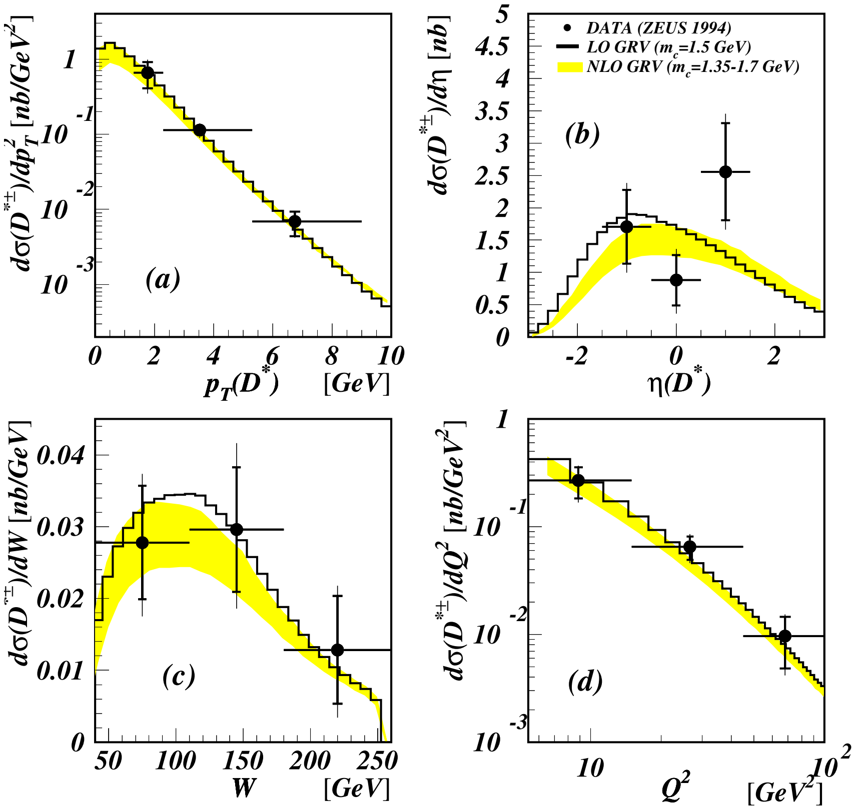


Figure 10: Differential cross sections for deep inelastic $D^*$ production.

## 6 Conclusion

Jets and heavy quarks carry the information from the partonic interactions in $ep$ collisions. The new HERA results in this field as discussed here can be successfully described in the framework of perturbative QCD. Due to the large kinematic range at HERA, complementary concepts have to be applied. Charm quarks appear as massive products of boson gluon fusion – or as massless partons in the proton and even the photon. Virtual photons can be considered as point-like probes of the hadron structure, but they also reveal their nature as composite hadronic objects as it is well explored now for their real counterpart. It is this variety in the HERA phenomenology that holds the promise of providing keys to new dimensions in our understanding of the strong interaction.

**Acknowledgments**

It is a pleasure to thank my colleagues in the H1 and ZEUS collaboration for providing the results for this review. I benefitted from conversations with B. Kniehl. I would like to thank B. Foster and his team for creating the stimulating atmosphere of the conference, and for the warm welcome I enjoyed at Bristol.

**References**

1. M. Martínez, Jet Shapes at HERA, talk at "DIS 97", Chicago, 1997, to appear in the proceedings.
2. T. Sjöstrand, CERN-TH-6488 (1992), Comp. Phys. Comm. 82 (1994) 74.
3. R. Akers *et al.* (OPAL Coll.), Z. Phys. C 63 (1994) 197.
4. F. Abe *et al.* (CDF Coll.), Phys. Rev. Lett. 70 (1993) 713,
   S. Abachi *et al.* (D0 Coll.), Phys. Lett. B357 (1995) 500.
5. M. Klasen, G. Kramer, Phys. Rev. D56 (1997) 2702.
6. M. Derrick *et al.* (ZEUS Coll.), Phys. Lett. B 384 (1996) 401.
7. B.W. Harris, J.F. Owens, Phys. Rev. D56 (1997) 4007.
8. T. Ahmed *et al.* (H1 Coll.). N. Phys. B445 (1995) 195.
9. C. Adloff *et al.* (H1 Coll.), preprint DESY 97-164.
10. B.L.Combridge, C.J.Maxwell, Nucl. Phys. B239 (1984) 429.
11. M. Glück, E. Reya, A. Vogt, Phys. Rev. D46 (1992) 1973.
12. H. Rick (H1 Coll.), PhD thesis, Universität Dortmund, Germany, 1997.
13. Ch. Berger *et al.* (PLUTO Coll.), Nucl. Phys. B281 (1987) 365;
    W. Bartel *et al.* (JADE Coll.), Z. Phys. C24 (1984) 231;
    M. Althoff *et al.* ( TASSO Coll.), Z. Phys. C31 (1986) 527;
    H. Aihara *et al.* (TPC/Two-Gamma Coll.), Z. Phys. C34 (1987) 1;
    S.K. Sahu *et al.* (AMY Coll.), Phys. Lett. B346 (1995) 208;
    K. Muramatsu *et al.* (TOPAZ Coll.), Z. Phys. C31 (1986) 527;
    P. Abreu *et al.* (DELPHI Coll.), Z. Phys. C69 (1996) 223;
    R. Akers *et al.* (OPAL Coll.), CERN-PPE/93-156, August 1993.
14. J.H. Field, F. Kapusta, L. Poggioli, Z. Phys. **C36** (1987) 121
15. J. Spiekermann, talk at "32nd Rencontres de Moriond: QCD and high-energy hadronic interactions", Les Arcs, France, 1997, to appear in the proceedings.
16. L. Lönnblad, Comp. Phys. Comm. 71 (1992) 15.
17. G.Ingelman, in: Proc. "Physics at HERA", Hamburg, 1991, eds. W. Buchmüller, G. Ingelman, Vol. 3;
    G. Ingelman, A. Edin, J. Rathsman, Comp. Phys. Comm. 101 (1997) 108.

18. S. Catani, M. Seymour, Nucl. Phys. B485 (1997) 291.
19. G. Schuler, T. Sjöstrand, Z. Phys. C68 (1995) 607, Phys. Lett. B 376 (1996) 193;
M. Glück, E. Reya, M. Stratman, Phys. Rev. D54 (1996) 5515.
20. M. Drees, R. Godbole, Phys. Rev. D50 (1994) 3124.
21. F. Borzumati, G. Schuler, Z. Phys. C58 (1993) 139.
22. C. Adloff *et al.* (H1 Collaboration), preprint DESY 97-164.
23. G. Marchesini et al., Comp. Phys. Comm. 67 (1992) 465.
24. A. Donnachie, P.V. Landshoff, Phys. Lett. B348 (1995) 213, ibid. B296 (1992) 227.
25. M.G. Ryskin, Z. Phys. C57 (1993) 89;
M.G. Ryskin, R.G. Roberts, A.D. Martin, E.M. Levin preprint DTP/95/96 CBPF-NF-079/95, RAL-TR-95-065, revised February 1996.
26. A. Meyer, talk at "5th Topical Seminar on the Irresistible Rise of the Standard Model", San Miniato, Italy, 1997, to appear in the proceedings.
27. S. Aid et al. (H1 Coll.), Nucl. Phys. B472 (1996) 3, and "Diffractive and non-diffractive photoproduction of $J/\Psi$ mesons at HERA", contr. paper to ICHEP 1996, Warsaw;
J. Breitweg *et al.* (ZEUS Coll.), Z. Phys. C75 (1997) 215, and preprint DESY 97-147.
28. A.D. Martin, R.G. Roberts, W.J. Stirling, Phys. Lett. B354 (1995) 155.
29. L.P.A. Haakman, A.Kaidalov, J.H. Koch, Phys. Lett. B365 (1996) 411;
L.L. Jenjovszky, E.S. Martynov, F. Paccanoni, Novy Svet Hadrons (1996) 170.
30. E.L. Berger, D. Jones, Phys. Rev. D23 (1981) 1521,
R. Baier, R. Rückl, Nucl. Phys. B201 (1982) 1.
31. M. Krämer, J. Zunft, J. Steegborn, P.M. Zerwas, Phys. Lett. B348 (1995) 657; M. Krämer, Nucl. Phys. B459 (1996) 3.
32. B.A. Kniehl, G. Kramer, preprints DESY-97-036, DESY-97-110.
33. F. Abe et al. (CDF Coll.), Phys. Rev. Let. 69 (1992) 3704;
A. Sansoni et al. (CDF Coll.), Nuovo Cim. 109A (1996) 827.
34. G.T. Bodwin, E. Braaten, G.P. Lepage, Phys. Rev. D51 (1995) 1125.
35. P. Cho, A.K. Leibovich, Phys. Rev. D53 (1996) 150, Phys. Rev. D53 (1996) 6203.
36. M. Cacciari, M. Krämer, Phys. Rev. Lett.76 (1996) 4128.
37. B. Cano-Coloma, M.A. Sanchis-Lozano, Valencia Univ. preprint IFIC-97-29, hep-ph/9706270.
38. M. Derrick et al. (ZEUS Coll.), Phys. Lett. B349 (1995) 225;
S. Aid *et al.* (H1 Coll.), Nucl. Phys. B472 (1996) 32.

39. C. Coldewey, talk at Ringberg Workshop on new trends in HERA physics, Ringberg, Germany, 1997, to appear in the proceedings.
40. S. Frixione et al., Phys. Lett. B348 (1995) 633, Nucl. Phys. B454 (1995) 3.
41. B.A. Kniehl, G. Kramer, M. Spira, preprint DESY-96-210;
J. Binnewies, B.A. Kniehl, G. Kramer, preprint DESY-97-012.
42. M. Cacciari, M. Greco, Phys. Rev. D55 (1997) 7134.
43. C. Peterson, D. Schlatter, I. Schmitt, P.M. Zerwas, Phys. Rev. D 27 (1983) 105.
44. J. Chrin, Z. Phys. C 36 (1987) 163.
45. B.W. Harris, J. Smith, Nucl. Phys. B452 (1995) 109; Phys. Lett. B353 (1995) 535; preprint DESY 97-111.
46. C. Adloff *et al.* (H1 Collaboration), Z. Phys. C72 (1996) 593;
J. Breitweg *et al.* (ZEUS Coll.), preprint DESY 97-089.